Microporous and Mesoporous Materials 328 (2021) 111450

Contents lists available at ScienceDirect

Microporous and Mesoporous Materials

journal homepage: www.elsevier.com/locate/micromeso

Optimizing bromide anchors for easy tethering of amines, nitriles and thiols in porous organic polymers towards enhanced CO_2 capture

Vepa Rozyyev [a,b], Mustafa S. Yavuz [b,c], Damien Thirion [b], Thien S. Nguyen [d,e], Thi Phuong Nga Nguyen [d], Abdul-Hamid Emwas [f], Cafer T. Yavuz [b,d,e,*]

[a] Pritzker School of Molecular Engineering, The University of Chicago, 5640 South Ellis Avenue, Chicago, IL, 60637, USA
[b] Graduate School of EEWS, KAIST, 291 Daehak-ro, Yuseong-gu, Daejeon, 34141, Republic of Korea
[c] Innvotek Limited, 43 Berkeley Square, Mayfair, London, W1J 5FJ, UK
[d] Advanced Membranes and Porous Materials Center (AMPM), Physical Science and Engineering (PSE), King Abdullah University of Science and Technology (KAUST), Thuwal, 23955-6900, Saudi Arabia
[e] KAUST Catalysis Center (KCC), Physical Science & Engineering (PSE), King Abdullah University of Science and Technology (KAUST), Thuwal, 23955, Saudi Arabia
[f] Core Labs, King Abdullah University of Science and Technology (KAUST), Thuwal, 23955-6900, Saudi Arabia

ARTICLE INFO

Keywords:
Carbon capture
Microporous materials
Surface post-functionalization
Amine tethering
Flue gas separation

ABSTRACT

Porous organic polymers with labile leaving groups offer direct access to reactive functional groups, otherwise not permissible during network formation. In a one-step, open air, self-coupling reaction of tris bromomethyl benzene, we report highly porous, bromine rich C–C bonded porous polymers. Due to the steric nature of the monomer, restrictive crosslinking allowed pendent bromine groups to remain unreacted and provided rapid exchange into amines, nitriles, and thiols. This simple but powerful strategy yielded two isostructural but varying porosity and pendent group density polymers, allowing a comparative gas uptake study. Despite having lower surface area, the porous polymer formed at low temperature showed higher amination due to higher density of bromine groups. The polymers with more pendant groups resulted better CO_2 uptake performances than higher porosity polymers with less pendant groups. Although post-modification decreased surface area of materials, amine functionalization greatly improved the CO_2 uptake capacity. The ethylenediamine appended version exhibited 4.7 times increase in CO_2 uptake capacity with highest CO_2/N_2 selectivity of 729 (298 K), and with an isosteric heat of 97 kJ mol^{-1} at zero coverage.

1. Introduction

Carbon dioxide recovery and storage is essential for curbing global warming, but current capture technologies are not yet optimized for low cost, scalable applications [1–3]. Solid nanoporous adsorbents such as metal organic frameworks (MOFs) [4–8], microporous organic polymers (MOPs) [9–12], and covalent organic polymers (COPs) [13–15] have been investigated as promising CO_2 adsorbents because they offer tunable pore sizes and functionalities, high surface areas, and low regeneration energy. The surface chemistry (i.e. functional moieties) dictates the strength of CO_2 binding, which is commonly estimated from isosteric heat of adsorption (Q_{st}). Stronger CO_2 binding gives both higher adsorption capacity and higher selectivity over nitrogen, the other but major component of flue gas [14,16–18]. Functional groups such as hydroxyl, carboxylic acid, sulfonic acid, sulfide, phosphonium and a number of nitrogen-based moieties such as alkylamines, aromatic amines, amidoximes, benzimidazole, and azo groups have been successfully studied for CO_2 capture [19–23]. Among these, alkylamines exhibit strongest binding to CO_2 via chemisorptive carbamate formation [15,24–26]. Alkylamine incorporated porous materials were reported to have Q_{st} values as high as 100 kJ mol^{-1} and CO_2/N_2 selectivities in the order of thousands [15,18,24]. The effect of amine surface density on CO_2 adsorption performance was also studied on porous materials such as mesoporous silica [27,28], and amine modified polystyrene polymer [29]. Majority of nanoporous sorbents lack the surface adsorption sites like nitrogen-based moieties for selective CO_2 binding, which leads to much lower CO_2 adsorption capacities than desired. To gain more effective adsorbent capacity, the surface of the nanoporous networks

* Corresponding author. Advanced Membranes and Porous Materials Center (AMPM), Physical Sciences and Engineering (PSE), King Abdullah University of Science and Technology (KAUST), Thuwal, 23955-6900, Saudi Arabia.
E-mail address: cafer.yavuz@kaust.edu.sa (C.T. Yavuz).

https://doi.org/10.1016/j.micromeso.2021.111450
Received 23 May 2021; Received in revised form 8 September 2021; Accepted 17 September 2021
Available online 21 September 2021

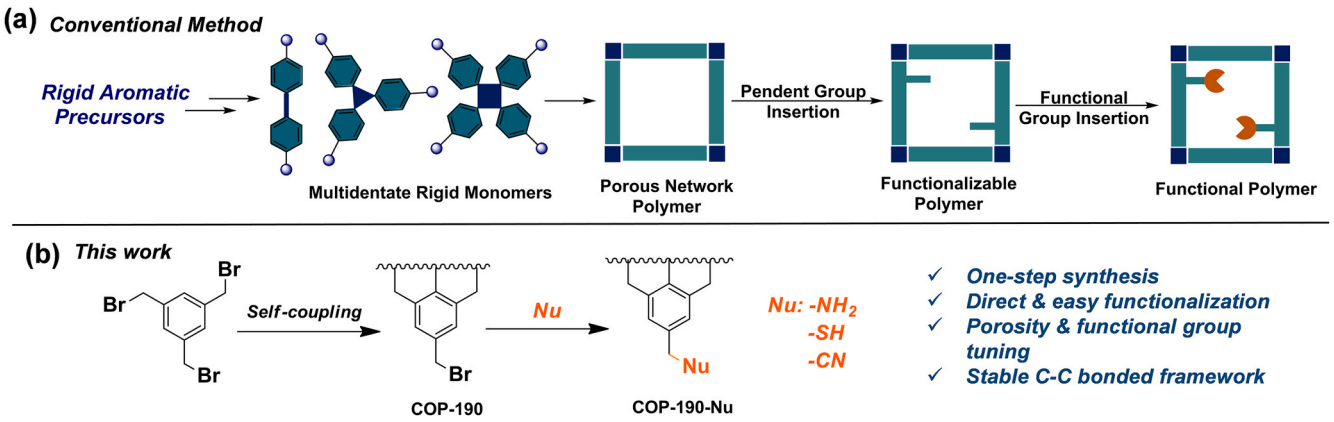

Scheme 1. (a) Conventional multi-step synthesis of functional nanoporous polymers. (b) Our one-step Friedel-Crafts synthesis of bromomethyl tethered porous network polymers and their S_N2 post-modification with CO_2-philic moieties.

should be derivatized with CO_2-philic moieties through post-modification techniques [30,31].

CO_2-philic moieties can be incorporated into porous materials by either physical impregnation or covalent bond formation through post-synthetic functionalization (Scheme 1) [32–34]. Covalently introducing functionalities has a significant advantage of higher thermal and chemical stability over impregnation [35–37]. But unlike homogeneous molecular synthesis, heterogeneous post-modification of nanoporous solids require tedious processing, concentrated reactive species, high temperatures, and prolonged reaction times for a successful grafting. Even then the process often fails to fully transform the solid due to mass transport limitations. Also, in every step of the modification, the surface areas of the materials decrease dramatically [14,15,18]. A compromise is to start with robust nanoporous polymers with C–C bonded frameworks, since they can withstand harsh conditions [38,39]. In comparison to others, Friedel-Crafts (FC) alkylation is one of the most promising methods when considering the vast availability of inexpensive precursors, and unsurprisingly used for generating nanoporous polymers having C–C bonded frameworks [9,40,41]. In a FC route, multifunctional benzyl halides with rigid frameworks are commonly used as monomers with anhydrous Lewis acid catalysts (e.g. $FeCl_3$) to form polymer networks. To obtain highly crosslinked and porous structure, the reactions are usually carried out at higher temperatures.

Here we report a new strategy based on FC self-coupling to prepare labile bromomethyl anchored C–C bonded nanoporous polymer networks in a single step without post-synthetic modification (Scheme 1). By varying the reaction temperature, the degree of crosslinking and the density of surface groups were tuned, which allowed us to study the effect of surface anchored group density on post-functionalization. Tethered bromomethyl groups were readily modified by bimolecular nucleophilic substitutions (S_N2) using ethylene diamine, diethylenetriamine, thiol and nitrile groups. The CO_2-philic moieties enhanced CO_2 adsorption capacity of the porous networks and resulted in higher Q_{st} values and CO_2/N_2 selectivities.

2. Experimental

2.1. Materials

Anhydrous iron (III) chloride ($FeCl_3$, 99.0%), sodium hydrosulfide hydrate (NaSH, 70%), 1,2-ethylene diamine (EN, 99.0%), 2,2′-diaminodiethylamine (98.5%, also named as diethylenetriamine, DETA), sodium cyanide (NaCN, 97.0%) were purchased from Samchun Pure Chemicals, Korea. 1,2-dichloroethane (DCE, 99.5%), methanol (MeOH, 99.8%) and chloroform ($CHCl_3$, 99.8%) were purchased from Daejung Chemicals, South Korea. 1,3,5-tris(bromomethyl)benzene (97%) was purchased from Sigma Aldrich, USA. Deionized water (DIW) was used from a Mili-Q (18.2 MQ·cm at 25 °C) system. Prior to use, 1,2-dichloroethane was dried and distilled over P_4O_{10} under nitrogen. All the other solvents and chemicals were used without further purification.

2.2. Experimental procedures

2.2.1. Synthesis of covalent organic polymer 190L (COP-190L)

2 mmol (735.84 mg, 356.88 g mol^{-1}) of 1,3,5-tris(bromomethyl) benzene was dissolved in 20 ml dry dichloroethane under N_2 atmosphere. 6 mmol (1.0 g, 162.2 g mol^{-1}) of anhydrous $FeCl_3$ was added to the solution. Reaction was stirred for 30 h at room temperature (RT). After the reaction, 20 ml MeOH was added to the flask to quench the excess $FeCl_3$. The precipitates were washed thoroughly with MeOH and then $CHCl_3$ until the filtrate was clear. The solid product, COP-190L, was dried under vacuum at 120 °C overnight. The dried mass of COP-190L was 398 mg (169% yield based on fully self-coupled polymer where no bromines are left unreacted).

2.2.2. Synthesis of COP-190H

2 mmol (735.84 mg, 356.88 g mol^{-1}) of 1,3,5-tris(bromomethyl) benzene was dissolved in 20 ml dry dichloroethane under N_2 atmosphere. 6 mmol (1.0 g, 162.2 g mol^{-1}) of anhydrous iron (III) chloride was added at once. Reaction was stirred for 30 h at 78 °C. After completion, the reaction mixture was allowed to cool to room temperature, and then 20 ml MeOH was added to the flask to quench the excess $FeCl_3$. The precipitate was washed with MeOH and $CHCl_3$ thoroughly until the filtrate was clear. The resultant solid was dried under vacuum at 120 °C overnight. The dried mass of COP-190H is 375 mg (159% yield based on fully self-coupled polymer where no bromines are left unreacted).

2.2.3. Synthesis of COP-190L-en, COP-190L-deta, COP-190H-en, and COP-190H-deta

200 mg of COP-190 was added into 50% (v/v) of 20 ml amine solution in acetonitrile, and the mixture was stirred at 100 °C for 48 h. The solids were filtered and washed for five times with MeOH and then washed thoroughly with water until the supernatant was neutral (monitored by a pH paper). The product was dried under vacuum at 120 °C overnight. The porous polymers are named as COP-190L-en and COP-190H-en for ethylenediamine (EN), COP-190L-deta and COP-190H-deta for diethylene triamine (DETA) grafted polymers.

2.2.4. Synthesis of COP-190H-CN and COP-190H-SH

200 mg of COP-190 and 500 mg of sodium cyanide (NaCN) or sodium hydrosulfide (NaHS) were added to the flask (sodium cyanide or sodium hydrosulfide was ground using mortar to make a fine powder). (***Caution: Both NaCN and NaSH are toxic, grind inside a fume hood,***

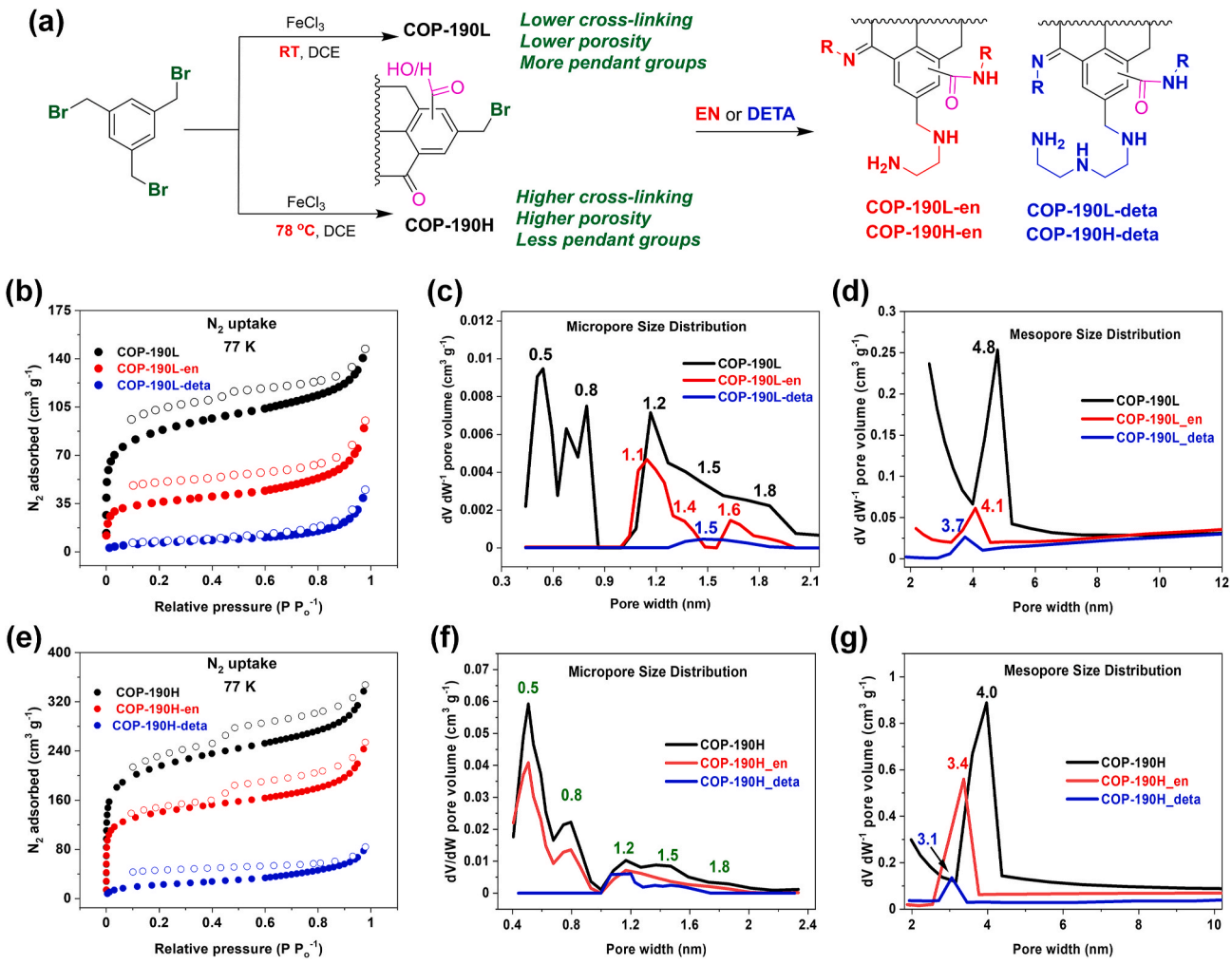

Fig. 1. (a) Synthesis of COP-190 and post-modification with ethylenediamine (EN) and diethylenetriamine (DETA). N_2 adsorption (solid circles) and desorption (empty circles) isotherms of (b) COP-190L, COP-190L-en, COP-190L-deta, and (e) COP-190H, COP-190H-en, COP-190H-deta at 77 K. Micropore size distributions of (c) COP-190L, COP-190L-en, COP-190L-deta, and (f) COP-190H, COP-190H-en, COP-190H-deta calculated using a NLDFT method. Mesopore size distributions of (d) COP-190L, COP-190L-en, COP-190L-deta, and (g) COP-190H, COP-190H-en, COP-190H-deta calculated using BJH method.

and always wear a proper mask during grinding). After adding 50 ml of DMF, the reaction mixture was stirred at 120 °C under nitrogen for 48 h. The reaction was quenched by slowly adding 30 ml of methanol, followed by filtering the solid and washing with water (15 ml each). The product was further sonicated in 6 M HCl for 30 min and soaked in HCl overnight. (***Caution: The acid addition process must be carried out inside a fume hood. Hydrogen sulfide and hydrogen cyanide byproducts are highly toxic. Wear a mask)*** The solid, once again, was filtered and thoroughly washed with water. The product was dried at 120 °C under vacuum for 12 h. The resulting polymers were named as COP-190H-CN for nitrile functionalization, and COP-190H-SH for thiol functionalization.

2.3. Characterization methods

Porosity characterization of polymers was carried out from nitrogen adsorption isotherms using a Micromeritics 3FLEX accelerated surface area and porosimetry analyzer at 77 K. Prior to measurement, samples were degassed at 423 K for 6 h under vacuum. The specific surface areas were derived from Brunauer-Emmett-Teller (BET) and Langmuir models. Micropore size distributions were calculated from adsorption data by a Micromeritics 3FLEX software using non-local density functional theory (NLDFT) with slit pores. Mesopore size distributions were calculated from desorption data by the Micromeritics 3FLEX software using a Barrett-Joyner-Halenda (BJH) method. The CO_2 and N_2 adsorption and desorption isotherms were measured at 273 K and 298 K by using a 3Flex surface characterization analyzer, Micromeritics Inc. Heat of adsorption data were calculated from CO_2 adsorption isotherms up to a pressure of 1.1 bar at 273 K and 298 K using Clausius-Clapeyron equation. The CO_2/N_2 selectivities were calculated according to the Ideal Adsorbed Solution Theory (IAST) for CO_2 (15%):N_2 (85%). The absolute component loadings were fitted with a single site Langmuir-Freundlich model.

Elemental composition was measured from energy-dispersive scanning (EDS) analysis of polymers on FEI Sirion scanning electron microscopy with an accelerated voltage of 10 kV. Fourier Transform Attenuated Total Reflectance-Infra-Red spectra (FT-ATR-IR) were recorded with a Shimadzu IRTracer, Gladi-ATR 10 model FTIR spectrometer. A sample (2–5 mg) was placed beneath the tip and over the laser and scanned for 20 times. Thermo-gravimetric analyses were performed on a Shimadzu DTG-60A by heating the samples from 30 °C up to 800 °C at a rate of 10 °C min^{-1} under air. Solid state CP-MAS ^{13}C NMR spectra were achieved on the 400 MHz Bruker Advance III spectrometer with the spinning speed of 14 kHz. The SEM and EDS images were recorded on the FEI Magellan 400 scanning electron microscope. All samples were sputter coated with 5 nm-thick Iridium layer before being observed top surface and elemental mapping in a scanning electron microscope (Magellan 400, FEI, USA) at accelerating voltage of 20

Table 1
Summary of gas adsorption data and elemental composition of COP-190 derivatives.

Materials	BET_{SA} ($m^2\ g^{-1}$)	$Lang_{SA}$ ($m^2\ g^{-1}$)	V_{total} ($cm^3\ g^{-1}$)	V_{micro} ($cm^3\ g^{-1}$)	CO_2 uptake at 298 K (mmol g^{-1})		Elemental composition (weight %)				
Conditions	77 K, N_2	77 K, N_2	0–60 nm	0–2 nm	0.15 bar	1 bar	C	N	O	S	Br
COP-190L	284	334	0.10	0.08	0.25	0.94	51.4	–	6.9	–	41.7
COP-190L-en	119	136	0.12	0.04	1.18	2.26	76.2	5.6	10.4	–	7.7
COP-190L-deta	22	28	0.036	0.0014	0.63	1.41	77.3	5.9	9.7	–	6.9
COP-190H	787	839	0.23	0.21	0.42	1.58	65.2	–	8.8	–	26.0
COP-190H-en	456	494	0.142	0.137	0.89	2.19	83.3	3.4	8.7	–	4.6
COP-190H-deta	72	80	0.047	0.011	0.72	1.79	83.8	3.7	9.0	–	3.5
COP-190H-CN	661	709	0.21	0.20	0.61	2.11	73.6	5.0	13.2	–	8.2
COP-190H-SH	773	827	0.25	0.23	0.61	2.28	72.5	–	10.8	7.7	9.0

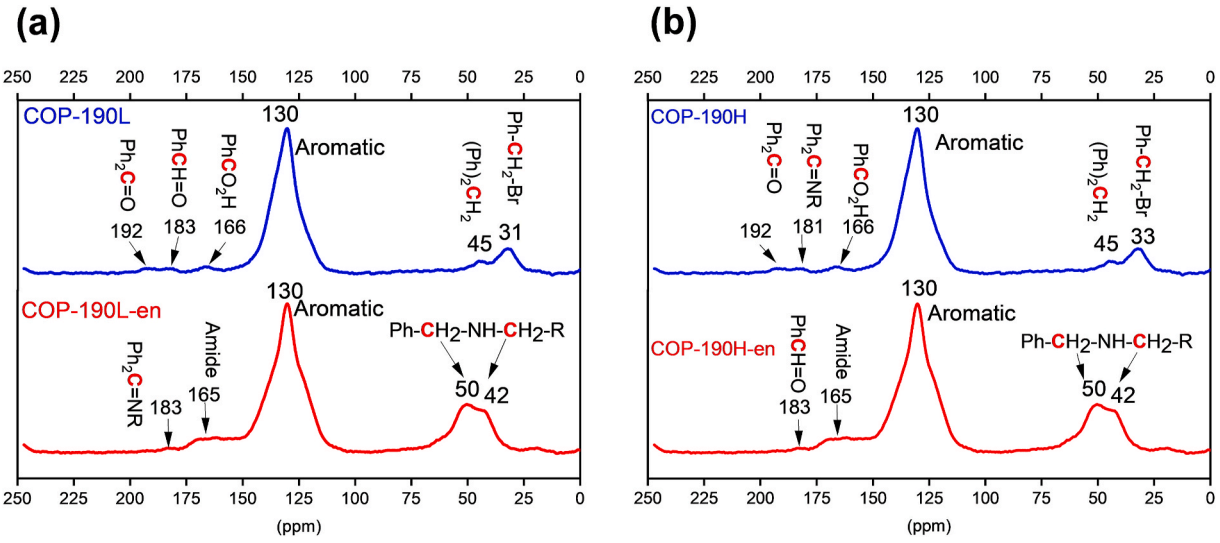

Fig. 2. Solid-state ^{13}C NMR spectra of COP-190 derivatives before and after ethylenediamine (en) functionalization. (a) COP-190L and COP-190L-en, (b) COP-190H and COP-190H-en.

kV.

3. Results and discussion

3.1. Synthesis and characterization of COP-190L and COP-190H

In a one-step procedure, a commercially available 1,3,5-tris(bromomethyl)benzene was self-coupled to produce covalent organic polymer (COP-190), through a FC alkylation in the presence of $FeCl_3$ (Fig. 1). Hypothetically, a fully self-crosslinked 1,3,5-tris(bromomethyl)benzene would have all core benzene molecules to be substituted at all six carbon positions with benzyl molecules, which is sterically and energetically unfeasible. Therefore, the network polymer, inadvertently, will contain unreacted benzyl bromides that can be functionalized by a rapid S_N2 reaction to incorporate new functional groups. COP-190 was synthesized at 78 °C named as COP-190H ("H" for high temperature), and at room temperature as COP-190L ("L" for low temperature) (Fig. 1). High temperature synthesis produced higher crosslinking and porosity, but less pendent groups. In contrast, lower temperature synthesis gave lower porosity but more pendent groups.

The porosities of synthesized COP-190 networks were studied using nitrogen (N_2) adsorption isotherms at 77 K (Fig. 1, S1-S3) and the results are summarized in Table 1. As anticipated, COP-190H showed a high Brunauer-Emmett-Teller (BET) surface area of 787 $m^2\ g^{-1}$ and total pore volume of 0.23 $cm^3\ g^{-1}$, while COP-190L showed only 284 $m^2\ g^{-1}$ and 0.10 $cm^3\ g^{-1}$. Both materials exhibited mesoporous and microporous morphologies, but COP-190H has more microporous structure. COP-190H possesses 91 wt % microporous volume while COP-190L showed only 80 wt %. Elemental composition of COP-190L revealed 41.7 wt % of bromine, while COP-190H has only 26.0 wt %, confirming that lower temperature synthesis forms products with more unreacted bromines (Table 1). Elemental analysis also revealed appearance of oxygen pendent groups on both COP-190L and COP-190H. Oxygen was likely introduced through hydrolysis of benzyl bromide, and oxidation of benzyl alcohol and aromatic C–H species, with the help of Lewis acid and oxidant $FeCl_3$. Broad O–H stretching band around 3400 cm^{-1} in FTIR spectra also confirms the presence of R–OH species in the synthesized polymers (Figs. S4 and S5). Solid-state ^{13}C NMR spectroscopy measurements of pristine COP-190H and COP-190L polymers show characteristic aromatic carbon peaks around 130 ppm, and aliphatic peaks of cross-linked $–CH_2-$ at 45 ppm, and unreacted $–CH_2$-Br at 33 ppm (Fig. 2). In addition, spectra also revealed small peaks at 192 ppm (ketone), 183 ppm (aldehyde), and 166 ppm (carboxylic acid), supporting the findings of elemental analysis and FTIR measurements.

3.2. Amine functionalization of COP-190L and COP-190H

COP-190L and COP-190H were then reacted with ethylenediamine (EN) to afford COP-190L-en and COP-190H-en, and with diethylenetriamine (DETA) to give COP-190L-deta and COP-190H-deta (Fig. 1a). The post-modified porous polymers exhibit characteristic N-H stretching at 3300 cm^{-1}, NH_2 bending band at 1650 cm^{-1}, C–N stretching at 1280 cm^{-1}, C–H stretching at 2900 cm^{-1}, and CH_2 bending around 1380 cm^{-1} (Fig. S4 and Fig. S5). After amination, bromine content decreases dramatically confirming the substitution reaction, but small fraction of bromine still left unreacted on COP-190 networks (Table 1). In COP-190L, bromine content drops from 41.7 wt % to 7.7 wt % and 6.9 wt % for COP-190L-en and COP-190L-deta, respectively. On the other hand,

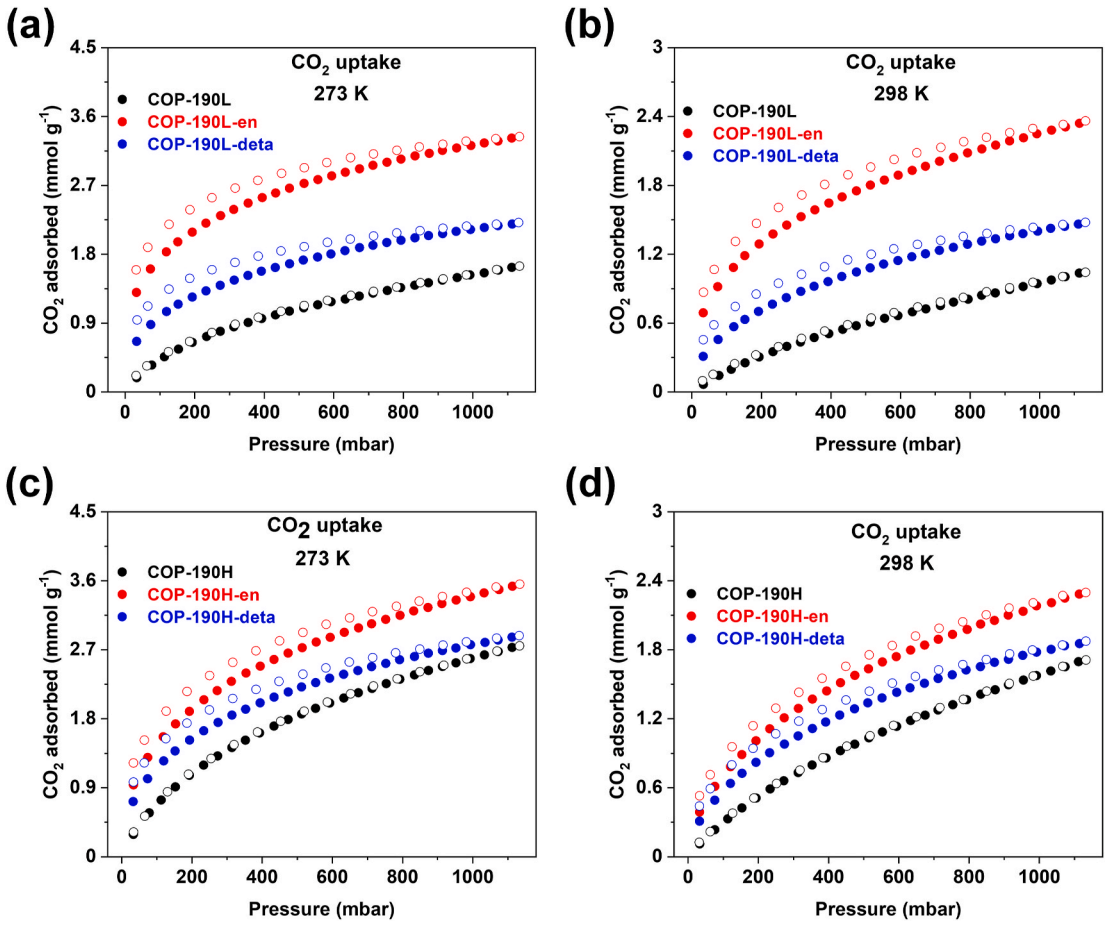

Fig. 3. CO_2 adsorption (solid circles) and desorption (empty circles) isotherms. COP-190L, COP-190L-en, and COP-190L-deta at (a) 273 K, and (b) 298 K. COP-190H, COP-190H-en, and COP-190H-deta at (c) 273 K, and (d) 298 K.

in COP-190H, bromine content drops from 26.0 wt % to 4.6 for COP-190H-en and to 3.5 wt % for COP-190H-deta. Also, due to the more bromomethyl anchoring groups available in COP-190L, more EN and DETA were introduced, evidenced by 5.6 wt % nitrogen in COP-190L-en, 5.9 wt % nitrogen in COP-190L-deta as compared to 3.4 wt % nitrogen in COP-190H-en, and 3.7 wt % nitrogen in COP-190H-deta. Thermogravimetric analysis of both amine modified and unmodified COP-190 derivatives show similar thermal stabilities up to the 300 °C, suggesting amines are covalently bonded rather than impregnated to the surface (Fig. S7). In addition, in both modified and unmodified COP-190, due to the desorption of adsorbed water, there is a 10–13 wt % mass loss up to 120 °C, which is common for nanoporous polymer networks [42,43].

One of the main challenges in post-synthetic functionalization of the nanoporous polymer networks is pore filling or clogging that causes significant loss in porosity [44]. Here, we investigated the change in pore size distribution (PSD) before and after the amine post-modification reaction and observed that not only size of reacting amines but also the density of surface anchoring groups affects the porosity of resulting material (Fig. 1). After diethylenetriamine (DETA) reaction, the pores at 0.5 nm and 0.8 nm disappeared for both COP-190L-deta and COP-190H-deta, respectively, suggesting pore filling by attached groups. When using smaller molecule than diethylenetriamine, such as ethylenediamine (EN), 0.5 nm and 0.8 nm pores were blocked in COP-190L-en, but COP-190H-en showed only small decrease in pore volume. Similarly, the pores at 1.2 nm vanished after post-amination of COP-190L-deta, but only small decrease in pore volume is observed in COP-190H-deta. We attribute this to lower density of anchoring bromomethyl groups in COP-190H, where pore volumes and sizes are affected less. The pores at 1.2, 1.5, 1.8 nm for both COP-190L and COP-190H, at 4.8 nm for COP-190L and at 4.0 for COP-190H shrunk in size and exhibited decrease in volume. In COP-190L with more anchoring groups, the reduction in pore size and volume is much higher. We also noticed higher decrease in pore sizes for larger pores as opposed to smaller ones. For instance, after EN functionalization of COP-190L, the pores at 4.8 nm shrunk by 0.7 nm, while pores at 1.8 nm shrunk by only 0.2 nm. We believe this is due to the different density of anchoring groups on different pore sizes or infiltration of amines into the smaller pores are harder than the larger ones. Smaller pores are formed as a result of higher crosslinking with lower density tethering groups in the vicinity.

3.3. *The CO_2 adsorption study of amine functionalized COP-190L and COP-190H*

In CO_2 adsorption capacity, both surface chemistry and porosity are known to play major roles [1]. Although introduction of amine groups enhances CO_2 adsorption, decrease in surface area usually has an adverse effect in performance. BET surface area of COP-190L dropped from 284 $m^2\ g^{-1}$ to 119 $m^2\ g^{-1}$ for COP-190L-en and to 22 $m^2\ g^{-1}$ for COP-190L-deta, and COP-190H surface area dropped from 787 $m^2\ g^{-1}$ to 456 $m^2\ g^{-1}$ for COP-190H-en, and to 72 $m^2\ g^{-1}$ for COP-190H-deta (Table 1). Despite significant losses in porosities, CO_2 adsorption performances greatly improved and COP-190L having more anchored groups showed greater improvement than COP-190H with less substitution. For instance, at 298 K and 0.15 bar, the relevant conditions for CO_2 capture from flue gas, adsorption capacity of COP-190L increased 4.7 times from 0.25 mmol/g to 1.18 mmol/g in COP-190L-en, but capacity of COP-190H only increased 2.1 times from 0.42 mmol/g to 0.89

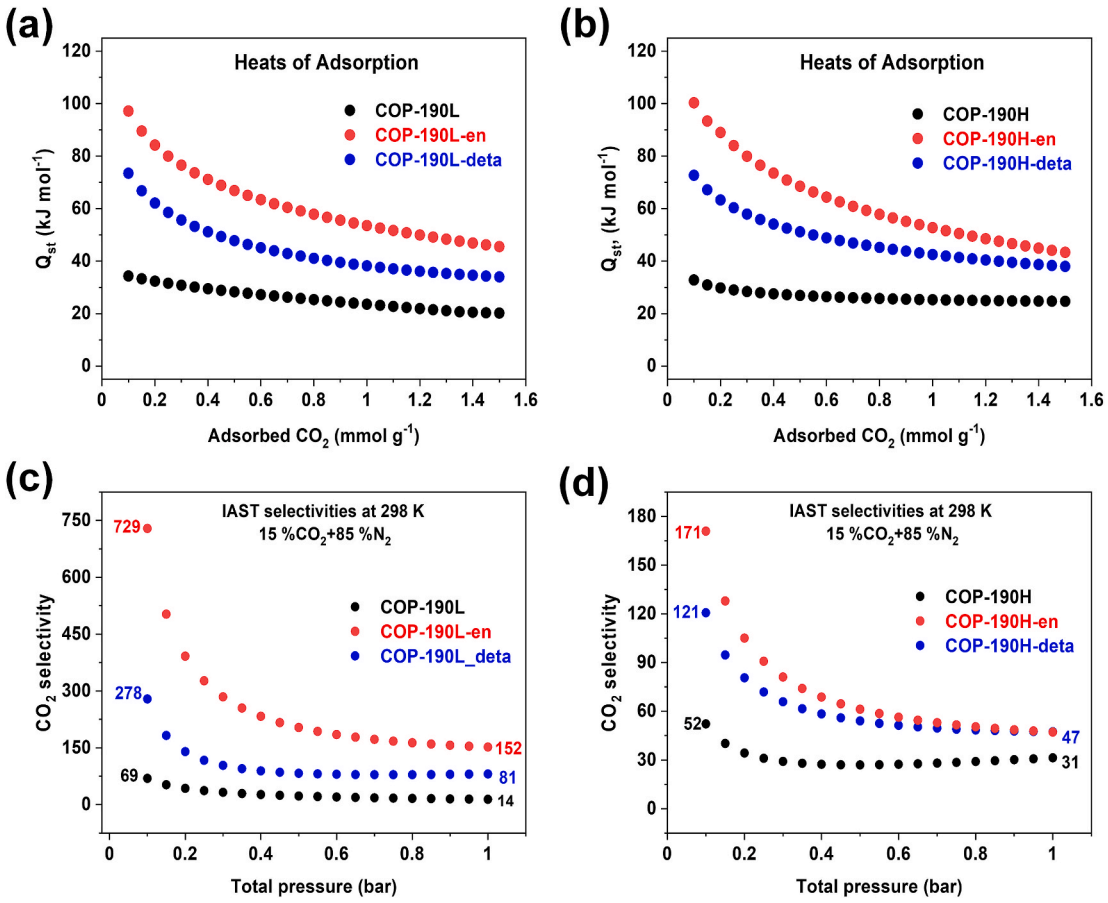

Fig. 4. CO_2 heats of adsorption data for (a) COP-190L, COP-190L-en, and COP-190L-deta, (b) COP-190H, COP-190H-en, and COP-190H-deta. IAST CO_2/N_2 (15:85) selectivities for (c) COP-190L, COP-190L-en, and COP-190L-deta, (d) COP-190H, COP-190H-en, and COP-190H-deta.

mmol/g in COP-190H-en (Table 1 and Fig. 3). Although EN and DETA modified derivatives have similar nitrogen contents, DETA derivatives gave lower CO_2 uptake which is, most likely, due to lower surface area.

The adsorption performance of the porous materials primarily depends on (1) porosity (surface area, size of the pores), and (2) nature and (3) density of surface chemistry. With the surface chemistry being similar, due to the higher porosity, COP-190H exhibited a higher CO_2 adsorption capacity than COP-190L. In the same way, COP-190L-en showed a higher capacity than COP-190L-deta, and COP-190H-en having a greater capacity than COP-190H-deta. However, the density of surface adsorptive functional group was observed to outweigh the porosity when the less porous COP-190L-en exhibited a higher adsorption capacity than COP-190H-en. On the other hand, in the low porosity regime, the difference in surface area became the determining factor as demonstrated by the higher capacity of COP-190H-deta (72 m^2/g, 0.72 mmol/g at 0.15 bar) than COP-190L-deta (22 m^2/g, 0.63 mmol/g at 0.15 bar). Among these materials, COP-190L-en showed best CO_2 adsorption performance (1.18 mmol/g at 0.15 bar and 2.26 mmol/g at 1 bar), because it has relatively higher surface area (119 m^2/g) with higher density of amine functionalized surface.

After post-modification of COP-190 with amine molecules, chemisorption of CO_2 is apparent from rapid increase in uptake at lower pressures and the noticeable hysteresis in adsorption-desorption profiles (Fig. 3). CO_2 binding strength was estimated from Qst values using adsorption data collected at 273 K and 298 K (Fig. 4). Irrespective of different porosity and density of functional groups, COP-190 networks with the same type of chemistry showed similar Qst values, as expected. At zero coverage, parent COP-190L and COP-190H polymer exhibited Qst values of 34 kJ mol^{-1} and 31 kJ mol^{-1}, respectively. After EN modification, Qst values increased to 97 kJ mol^{-1} and 100 kJ mol^{-1} for COP-190L-en and COP-190H-en, respectively. After modifying with DETA, Qst increased to 73 kJ mol^{-1} for both COP-190L-deta and COP-190H-deta. These high values are the result of strong chemisorptive binding of CO_2 originated from incorporated amine functionalities.

CO_2/N_2 selectivity from a simulated flue gas mixture (15% CO_2 and 85% N_2) is vital in assessing the performance of adsorbents. Selectivities were calculated from CO_2 and N_2 adsorption isotherms at 298 K using IAST method for 15% CO_2 and 85% N_2 (Fig. 4). Both EN and DETA incorporation enhanced the selectivity of COP-190 derivatives. COP-190L with more anchored groups showed greater improvement than COP-190H, and EN modified COP-190 derivatives showed better improvement than DETA-modified ones. CO_2/N_2 selectivity increased from 69 to 729 (>10x) in COP-190L-en, and to 278 (>4x) for COP-190L-deta. In COP-190H having lower density of amines, selectivity increased from 52 to 171 (>3.2x) for COP-190H-en, and to 121 (>2.3x) for COP-190H-deta.

3.4. CO_2 adsorption study of thiol and nitrile functionalized COP-190H

Nanoporous materials with polar thiol and nitrile chemistries were reported to enhance CO_2 performance through weak physisorptive binding [45,46]. They are also found to be useful in water treatment applications [46,47]. We, therefore, studied both thiol and nitrile functionalization of COP-190H, and their CO_2 capture performances (Fig. 5). Sodium hydrosulfide and sodium cyanide were reacted with COP-190H through well-known S_N2 mechanisms to give COP-190H-CN (for nitrile) and COP-190H-SH (for thiol). Elemental analysis and FTIR spectra show successful nitrile and thiol functionalizations. After post-modification, 7.7 wt % sulfur was observed in COP-190H-SH, and bromine content decreased from 26.0 wt % to 9.0 wt % (Table 1). In

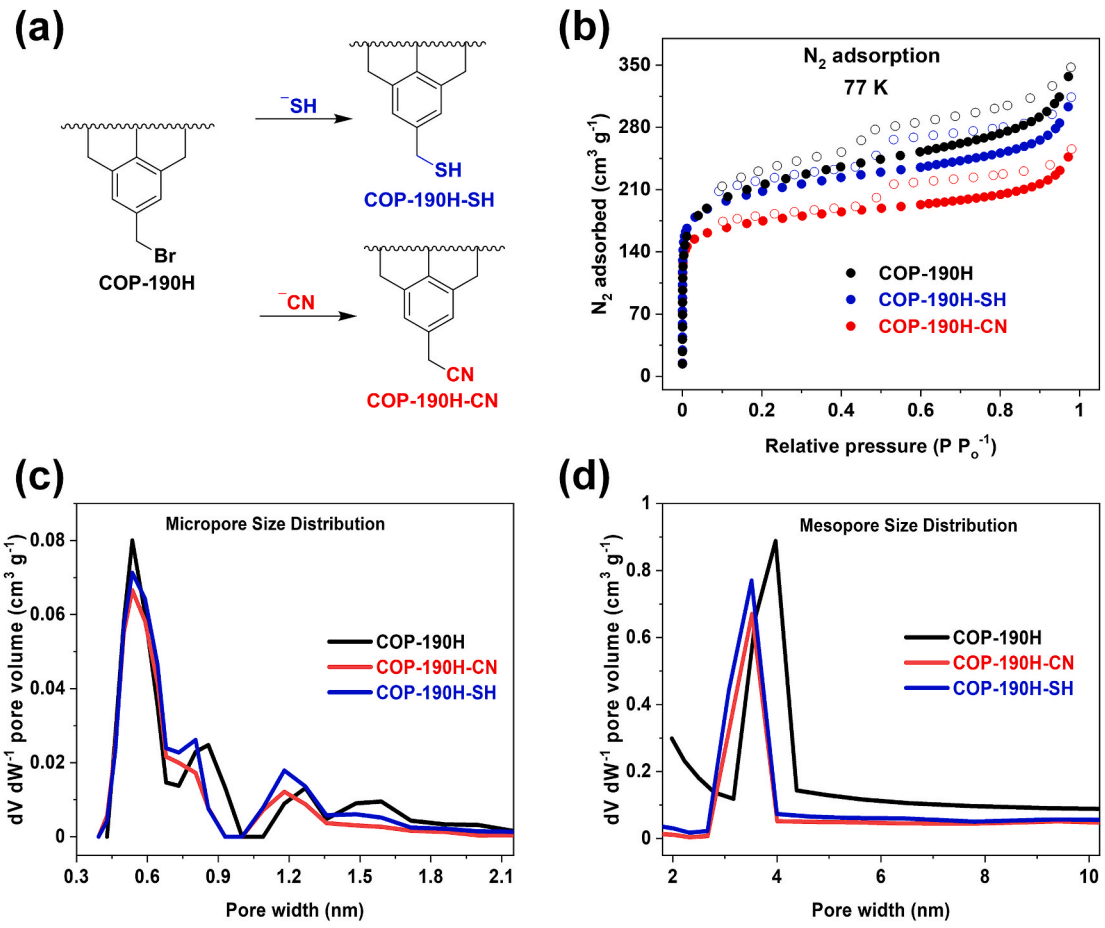

Fig. 5. (a) Nitrile (CN) and thiol (SH) functionalization of COP-190H. (b) N_2 adsorption (solid circles) and desorption (empty circles) isotherms of COP-190H, COP-190H-CN, and COP-190H-SH at 77 K. (c) Micropore size distributions for COP-190H, COP-190H-CN, and COP-190H-SH, calculated using NLDFT method. (d) Mesopore size distributions for COP-190H, COP-190L-CN, and COP-190L-SH, calculated using BJH method.

COP-190H-CN 5.0 wt % nitrogen was detected, and bromine content decreased to 9.0 wt %. Characteristic nitrile stretching at 2200 cm^{-1} is also evident in FTIR spectra of nitrile grafted COP-190H-CN (Fig. S6). Due to smaller size of thiol and nitrile groups, porosity is not expected to decrease as much as EN and DETA modified COP-190 networks. Indeed, COP-190H-SH and COP-190-CN exhibited BET surface areas of 773 m^2 g^{-1} and 661 m^2 g^{-1}, respectively, giving only 2% decrease for thiol and 16% decrease for nitrile (Fig. 5 and Table 1). Moreover, as expected, pores size distributions of COP-190H-SH and COP-190-CN were also not affected as much, showing only slight decrease in pore volume and size (Fig. 5). Incorporation of nitrile and thiol groups also improved the CO_2 capture performance, resulting higher adsorption capacities, Qst values, and CO_2/N_2 selectivities. Qst values increased from 31 kJ mol^{-1} to 42 kJ mol^{-1} in COP-190H-CN and to 37 kJ mol^{-1} in COP-190H-SH, and IAST CO_2/N_2 (15:85) selectivities increased from 52 to 76 for COP-190H-SH and to 91 for COP-190H-CN (Fig. 6). Although nitrile groups exhibited stronger binding energy than thiols, CO_2 adsorption capacity increased by only 26% in COP-190H-CN as compared to 41% in COP-190-SH (Fig. 6 and Table 1). We attribute this to the lower surface area of COP-190H-CN. Due to the weaker interaction of nitrile and thiol groups with CO_2, regardless of higher surface area, improvement in CO_2 uptake performances is much lower than EN and DETA functionalized COP-190 networks.

4. Conclusion

In summary, we have demonstrated a facile method to prepare nanoporous polymers with anchored benzyl bromides, and their post-modifications for enhanced CO_2 capture. Porosity and density of anchored groups were successfully tuned by changing the reaction temperature. Tethered bromides were substituted by amine molecules, ethylenediamine and diethylenetriamine, for improving CO_2 capture capabilities from flue gas mixture. Amine decorated COP-190 networks gave a significant improvement in CO_2 capacity, heat of adsorption, and CO_2/N_2 selectivity. COP-190L having more anchored bromomethyl groups showed greater improvement than COP-190H, and ethylenediamine pendent groups showed better improvement than diethylenetriamine ones. In addition, we have showed successful replacement of bromides to produce nitrile and thiol appended nanoporous COP-190 networks. Our results demonstrate the effect of surface functional group density on CO_2 adsorption performance, which leads to better understanding of sorbent properties. The ability to tune the surface functionality coverage of porous polymers may enable the synthesis of better sorbents for CO_2 separation from industrial flue gas mixtures. Furthermore, the one-step formation of a functional porous polymer with labile leaving groups provides tremendous opportunities for a wide range of applications such as vapor capture and catalysis, areas of which we're currently working on.

CRediT authorship contribution statement

Vepa Rozyyev: Methodology, Validation, Investigation, Formal analysis, Writing – original draft. **Mustafa S. Yavuz:** Investigation. **Damien Thirion:** Formal analysis. **Thien S. Nguyen:** Formal analysis, Writing – review & editing. **Thi Phuong Nga Nguyen:** Formal analysis. **Abdul-Hamid Emwas:** Formal analysis. **Cafer T. Yavuz:**

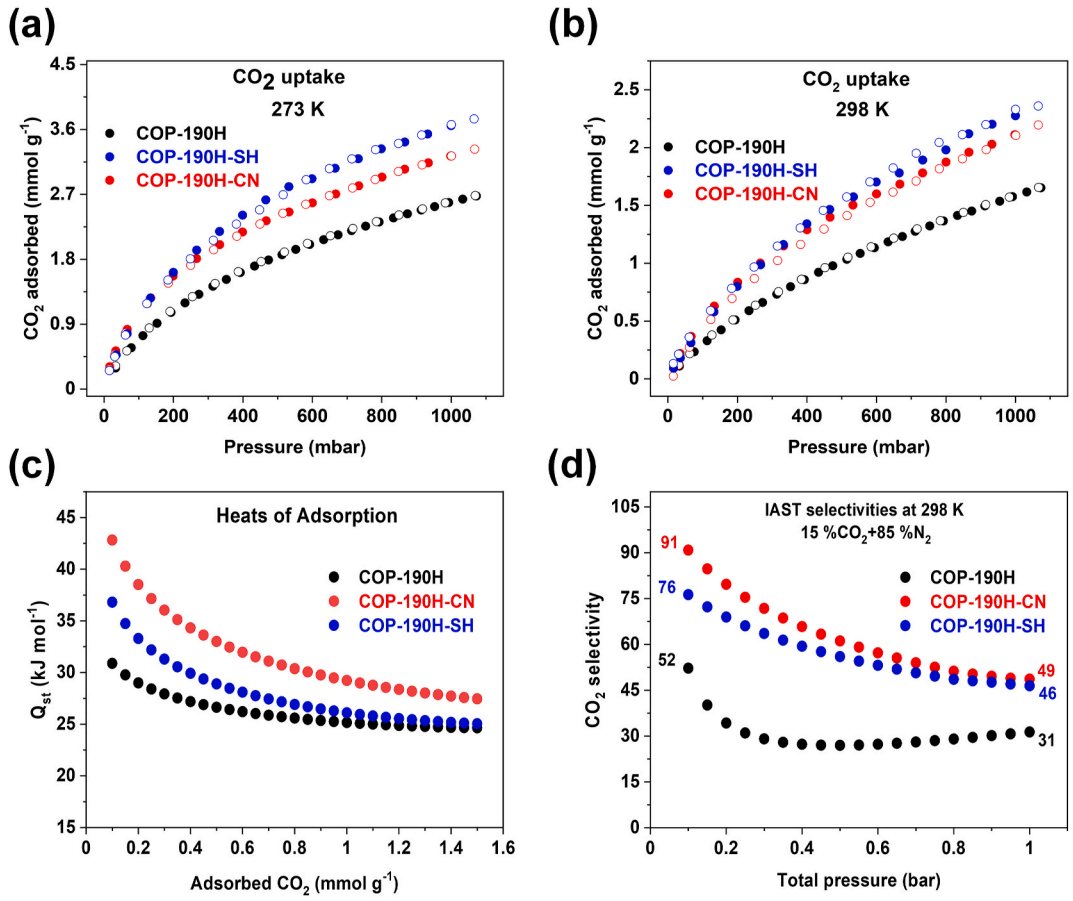

Fig. 6. CO_2 adsorption and desorption isotherms of COP-190H, COP-190H-CN, and COP-190H-SH at (a) 273 K, and (b) 298 K. (c) Heats of adsorption data for COP-190H, COP-190H-CN, and COP-190H-SH. (d) IAST CO_2/N_2 (15:85) selectivities for COP-190H, COP-190H-CN, and COP-190H-SH.

Conceptualization, Validation, Writing – original draft, Supervision, Project administration, Funding acquisition.

Declaration of competing interest

The authors declare that they have no known competing financial interests or personal relationships that could have appeared to influence the work reported in this paper.

Acknowledgments

This work was supported by National Research Foundation of Korea (NRF) grants funded by the Korean government (MSIP) (No. NRF-2017M3A7B4042140 and NRF-2017M3A7B4042235) and the startup funds by the King Abdullah University of Science and Technology (KAUST).

Appendix A. Supplementary data

Supplementary data to this article can be found online at https://doi.org/10.1016/j.micromeso.2021.111450.

References

[1] H.A. Patel, J. Byun, C.T. Yavuz, Carbon dioxide capture adsorbents: chemistry and methods, ChemSusChem 10 (2017) 1303–1317, https://doi.org/10.1002/cssc.201601545.
[2] A. Samanta, A. Zhao, G.K.H. Shimizu, P. Sarkar, R. Gupta, Post-Combustion CO2 capture using solid sorbents: a review, Ind. Eng. Chem. Res. 51 (2012) 1438–1463, https://doi.org/10.1021/ie200686q.
[3] K. Adil, P.M. Bhatt, Y. Belmabkhout, S.M.T. Abtab, H. Jiang, A.H. Assen, A. Mallick, A. Cadiau, J. Aqil, M. Eddaoudi, Valuing metal–organic frameworks for postcombustion carbon capture: a benchmark study for evaluating physical adsorbents, Adv. Mater. 29 (2017) 1702953, https://doi.org/10.1002/adma.201702953.
[4] T. Islamoglu, Z. Chen, M.C. Wasson, C.T. Buru, K.O. Kirlikovali, U. Afrin, M. R. Mian, O.K. Farha, Metal–organic frameworks against toxic chemicals, Chem. Rev. 120 (2020) 8130–8160, https://doi.org/10.1021/acs.chemrev.9b00828.
[5] D. Yancy-Caballero, K.T. Leperi, B.J. Bucior, R.K. Richardson, T. Islamoglu, O. K. Farha, F. You, R.Q. Snurr, Process-level modelling and optimization to evaluate metal–organic frameworks for post-combustion capture of CO2, Mol. Syst. Des. Eng. 5 (2020) 1205–1218, https://doi.org/10.1039/D0ME00060D.
[6] A. Aijaz, N. Fujiwara, Q. Xu, From metal–organic framework to nitrogen-decorated nanoporous carbons: high CO2 uptake and efficient catalytic oxygen reduction, J. Am. Chem. Soc. 136 (2014) 6790–6793, https://doi.org/10.1021/ja5003907.
[7] P. Pachfule, D. Shinde, M. Majumder, Q. Xu, Fabrication of carbon nanorods and graphene nanoribbons from a metal–organic framework, Nat. Chem. 8 (2016) 718–724, https://doi.org/10.1038/nchem.2515.
[8] V. Rozyyev, C.T. Yavuz, An all-purpose porous cleaner for acid gas removal and dehydration of natural gas, Chemistry 3 (2017) 719–721, https://doi.org/10.1016/j.chempr.2017.10.014.
[9] C. Xu, G. Yu, J. Yuan, M. Strømme, N. Hedin, Microporous organic polymers as CO2 adsorbents: advances and challenges, Mater. Today Adv. 6 (2020) 100052, https://doi.org/10.1016/j.mtadv.2019.100052.
[10] H. Wang, Z. Cheng, Y. Liao, J. Li, J. Weber, A. Thomas, C.F.J. Faul, Conjugated microporous polycarbazole networks as precursors for nitrogen-enriched microporous carbons for CO2 storage and electrochemical capacitors, Chem. Mater. 29 (2017) 4885–4893, https://doi.org/10.1021/acs.chemmater.7b00857.
[11] G. Zhu, H. Ren, Gas sorption using porous organic frameworks BT - porous organic frameworks, in: G. Zhu, H. Ren (Eds.), Design, Synthesis and Their Advanced Applications, Springer Berlin Heidelberg, Berlin, Heidelberg, 2015, pp. 57–85, https://doi.org/10.1007/978-3-662-45456-5_4.
[12] X. Gao, X. Zou, H. Ma, S. Meng, G. Zhu, Highly selective and permeable porous organic framework membrane for CO2 capture, Adv. Mater. 26 (2014) 3644–3648, https://doi.org/10.1002/adma.201400020.
[13] P. Jorayev, I. Tashov, V. Rozyyev, T.S. Nguyen, N.A. Dogan, C.T. Yavuz, Covalent amine tethering on ketone modified porous organic polymers for enhanced CO2 capture, ChemSusChem 13 (2020) 6433–6441, https://doi.org/10.1002/cssc.202002190.
[14] D. Thirion, V. Rozyyev, J. Park, J. Byun, Y. Jung, M. Atilhan, C.T. Yavuz, Observation of the wrapping mechanism in amine carbon dioxide molecular

interactions on heterogeneous sorbents, Phys. Chem. Chem. Phys. 18 (2016) 14177–14181, https://doi.org/10.1039/C6CP01382A.
[15] N.A. Dogan, E. Ozdemir, C.T. Yavuz, Direct access to primary amines and particle morphology control in nanoporous CO2 sorbents, ChemSusChem 10 (2017) 2130–2134, https://doi.org/10.1002/cssc.201700190.
[16] D.R. Kumar, C. Rosu, A.R. Sujan, M.A. Sakwa-Novak, E.W. Ping, C.W. Jones, Alkyl-aryl amine-rich molecules for CO2 removal via direct air capture, ACS Sustain. Chem. Eng. 8 (2020) 10971–10982, https://doi.org/10.1021/acssuschemeng.0c03706.
[17] V.Y. Mao, P.J. Milner, J.-H. Lee, A.C. Forse, E.J. Kim, R.L. Siegelman, C. M. McGuirk, L.B. Porter-Zasada, J.B. Neaton, J.A. Reimer, J.R. Long, Cooperative carbon dioxide adsorption in alcoholamine- and alkoxyalkylamine-functionalized metal–organic frameworks, Angew. Chem. Int. Ed. 59 (2020) 19468–19477, https://doi.org/10.1002/anie.201915561.
[18] W. Lu, J.P. Sculley, D. Yuan, R. Krishna, Z. Wei, H.-C. Zhou, Polyamine-tethered porous polymer networks for carbon dioxide capture from flue gas, Angew. Chem. Int. Ed. 51 (2012) 7480–7484, https://doi.org/10.1002/anie.201202176.
[19] J. Wang, J.G. Wei Yang, G. Yi, Y. Zhang, Phosphonium salt incorporated hypercrosslinked porous polymers for CO2 capture and conversion, Chem. Commun. 51 (2015) 15708–15711, https://doi.org/10.1039/C5CC06295K.
[20] M.G. Rabbani, H.M. El-Kaderi, Template-free synthesis of a highly porous benzimidazole-linked polymer for CO2 capture and H2 storage, Chem. Mater. 23 (2011) 1650–1653, https://doi.org/10.1021/cm200411p.
[21] H. Li, J. Li, A. Thomas, Y. Liao, Ultra-high surface area nitrogen-doped carbon aerogels derived from a schiff-base porous organic polymer aerogel for CO2 storage and supercapacitors, Adv. Funct. Mater. 29 (2019) 1904785, https://doi.org/10.1002/adfm.201904785.
[22] Z. Yang, S. Wang, Z. Zhang, W. Guo, K. Jie, M.I. Hashim, O.Š. Miljanić, D. Jiang, I. Popovs, S. Dai, Influence of fluorination on CO2 adsorption in materials derived from fluorinated covalent triazine framework precursors, J. Mater. Chem. A. 7 (2019) 17277–17282, https://doi.org/10.1039/C9TA02573A.
[23] Y. Belmabkhout, P.M. Bhatt, K. Adil, R.S. Pillai, A. Cadiau, A. Shkurenko, G. Maurin, G. Liu, W.J. Koros, M. Eddaoudi, Natural gas upgrading using a fluorinated MOF with tuned H2S and CO2 adsorption selectivity, Nat. Energy. 3 (2018) 1059–1066, https://doi.org/10.1038/s41560-018-0267-0.
[24] T.M. McDonald, D.M. D'Alessandro, R. Krishna, J.R. Long, Enhanced carbon dioxide capture upon incorporation of N,N′-dimethylethylenediamine in the metal–organic framework CuBTTri, Chem. Sci. 2 (2011) 2022–2028, https://doi.org/10.1039/C1SC00354B.
[25] K. Min, W. Choi, C. Kim, M. Choi, Oxidation-stable amine-containing adsorbents for carbon dioxide capture, Nat. Commun. 9 (2018) 726, https://doi.org/10.1038/s41467-018-03123-0.
[26] M.J. Al-Marri, M.M. Khader, E.P. Giannelis, M.F. Shibl, Optimization of selection of chain amine scrubbers for CO2 capture, J. Mol. Model. 20 (2014) 2518, https://doi.org/10.1007/s00894-014-2518-8.
[27] D.H. Jo, C.H. Lee, H. Jung, S. Jeon, S.H. Kim, Effect of amine surface density on CO2 adsorption behaviors of amine-functionalized polystyrene, Bull. Chem. Soc. Jpn. 88 (2015) 1317–1322, https://doi.org/10.1246/bcsj.20150123.
[28] B. Aziz, N. Hedin, Z. Bacsik, Quantification of chemisorption and physisorption of carbon dioxide on porous silica modified by propylamines: effect of amine density, Microporous Mesoporous Mater. 159 (2012) 42–49, https://doi.org/10.1016/j.micromeso.2012.04.007.
[29] P.D. Young, J.M. Notestein, The role of amine surface density in carbon dioxide adsorption on functionalized mixed oxide surfaces, ChemSusChem 4 (2011) 1671–1678, https://doi.org/10.1002/cssc.201100244.
[30] C. Wang, H. Luo, H. Li, X. Zhu, B. Yu, S. Dai, Tuning the physicochemical properties of diverse phenolic ionic liquids for equimolar CO2 capture by the substituent on the anion, Chem. Eur J. 18 (2012) 2153–2160, https://doi.org/10.1002/chem.201103092.
[31] W.M. Verdegaal, K. Wang, J.P. Sculley, M. Wriedt, H.-C. Zhou, Evaluation of metal-organic frameworks and porous polymer networks for CO2-capture applications, ChemSusChem 9 (2016) 636–643, https://doi.org/10.1002/cssc.201501464.
[32] M.J. Al-Marri, M.M. Khader, M. Tawfik, G. Qi, E.P. Giannelis, CO2 sorption kinetics of scaled-up polyethylenimine-functionalized mesoporous silica sorbent, Langmuir 31 (2015) 3569–3576, https://doi.org/10.1021/acs.langmuir.5b00189.
[33] J.M. Kolle, A. Sayari, Covalently immobilized polyethylenimine for CO2 adsorption, Ind. Eng. Chem. Res. 59 (2020) 6944–6950, https://doi.org/10.1021/acs.iecr.9b04669.
[34] L. Zou, Y. Sun, S. Che, X. Yang, X. Wang, M. Bosch, Q. Wang, H. Li, M. Smith, S. Yuan, Z. Perry, H.-C. Zhou, Porous organic polymers for post-combustion carbon capture, Adv. Mater. 29 (2017) 1700229, https://doi.org/10.1002/adma.201700229.
[35] C. Rosu, S.H. Pang, A.R. Sujan, M.A. Sakwa-Novak, E.W. Ping, C.W. Jones, Effect of extended aging and oxidation on linear poly(propylenimine)-mesoporous silica composites for CO2 capture from simulated air and flue gas streams, ACS Appl. Mater. Interfaces 12 (2020) 38085–38097, https://doi.org/10.1021/acsami.0c09554.
[36] W. Choi, J. Park, C. Kim, M. Choi, Structural effects of amine polymers on stability and energy efficiency of adsorbents in post-combustion CO2capture, Chem. Eng. J. 408 (2021) 127289, https://doi.org/10.1016/j.cej.2020.127289.
[37] M. Jahandar Lashaki, S. Khiavi, A. Sayari, Stability of amine-functionalized CO2 adsorbents: a multifaceted puzzle, Chem. Soc. Rev. 48 (2019) 3320–3405, https://doi.org/10.1039/C8CS00877A.
[38] O.T. Qazvini, S.G. Telfer, MUF-16: a robust metal–organic framework for pre- and post-combustion carbon dioxide capture, ACS Appl. Mater. Interfaces 13 (2021) 12141–12148, https://doi.org/10.1021/acsami.1c01156.
[39] T. İslamoğlu, M. Gulam Rabbani, H.M. El-Kaderi, Impact of post-synthesis modification of nanoporous organic frameworks on small gas uptake and selective CO2 capture, J. Mater. Chem. A. 1 (2013) 10259–10266, https://doi.org/10.1039/C3TA12305G.
[40] V. Rozyyev, D. Thirion, R. Ullah, J. Lee, M. Jung, H. Oh, M. Atilhan, C.T. Yavuz, High-capacity methane storage in flexible alkane-linked porous aromatic network polymers, Nat. Energy. 4 (2019) 604–611, https://doi.org/10.1038/s41560-019-0427-x.
[41] J. Huang, S.R. Turner, Hypercrosslinked polymers: a review, Polym. Rev. 58 (2018) 1–41, https://doi.org/10.1080/15583724.2017.1344703.
[42] T. Muangthong-on, J. Wannapeera, H. Ohgaki, K. Miura, TG-DSC study to measure heat of desorption of water during the thermal drying of coal and to examine the role of adsorption of water vapor for examining spontaneous heating of coal over 100 °C, Energy Fuel. 31 (2017) 10691–10698, https://doi.org/10.1021/acs.energyfuels.7b01836.
[43] Y. Byun, S.H. Je, S.N. Talapaneni, A. Coskun, Advances in porous organic polymers for efficient water capture, Chem. Eur J. 25 (2019) 10262–10283, https://doi.org/10.1002/chem.201900940.
[44] G. Qi, L. Fu, E.P. Giannelis, Sponges with covalently tethered amines for high-efficiency carbon capture, Nat. Commun. 5 (2014) 5796, https://doi.org/10.1038/ncomms6796.
[45] H.A. Patel, F. Karadas, J. Byun, J. Park, E. Deniz, A. Canlier, Y. Jung, M. Atilhan, C. T. Yavuz, Highly stable nanoporous sulfur-bridged covalent organic polymers for carbon dioxide removal, Adv. Funct. Mater. 23 (2013) 2270–2276, https://doi.org/10.1002/adfm.201202442.
[46] N.A. Dogan, Y. Hong, E. Ozdemir, C.T. Yavuz, Nanoporous polymer microspheres with nitrile and amidoxime functionalities for gas capture and precious metal recovery from E-waste, ACS Sustain. Chem. Eng. 7 (2019) 123–128, https://doi.org/10.1021/acssuschemeng.8b05490.
[47] D.J. Parker, H.A. Jones, S. Petcher, L. Cervini, J.M. Griffin, R. Akhtar, T. Hasell, Low cost and renewable sulfur-polymers by inverse vulcanisation, and their potential for mercury capture, J. Mater. Chem. A. 5 (2017) 11682–11692, https://doi.org/10.1039/C6TA09862B.